A Relativistic Quantum-Chemical Analysis of the trans Influence on 1H NMR Hydride Shifts in Square-Planar Platinum(II) Complexes

ARTICLE *in* INORGANIC CHEMISTRY · JULY 2015

Impact Factor: 4.76 · DOI: 10.1021/acs.inorgchem.5b00446

6 AUTHORS, INCLUDING:

Peter Hrobárik

Technische Universität Berlin

35 PUBLICATIONS **578** CITATIONS

Inorganic Chemistry

Article

pubs.acs.org/IC

A Relativistic Quantum-Chemical Analysis of the trans Influence on ^{1}H NMR Hydride Shifts in Square-Planar Platinum(II) Complexes

Anja H. Greif,[†] Peter Hrobárik,*[,†] Veronika Hrobáriková,[†] Alexei V. Arbuznikov,[†] Jochen Autschbach,[‡] and Martin Kaupp*[,†]

[†]Institut für Chemie, Technische Universität Berlin, Strasse des 17. Juni 135, 10623 Berlin, Germany

[‡]Department of Chemistry, University at Buffalo, State University of New York, Buffalo, New York 14260, United States

Supporting Information

ABSTRACT: Empirical correlations between characteristic ^{1}H NMR shifts in Pt(II) hydrides with trans ligand influence series, Pt−H distances, and ^{195}Pt shifts are analyzed at various levels of including relativistic effects into density-functional calculations. A close examination of the trans ligand effects on hydride NMR shifts is shown to be dominated by spin−orbit shielding σ^{SO}. A rather complete understanding of the trends has been obtained by detailed molecular orbital (MO)-by-MO and localized MO analyses of the paramagnetic and spin−orbit (SO) contributions to the chemical shifts, noting that it is the perpendicular shift-tensor components that determine the trend of the ^{1}H hydride shifts. In contrast to previous assumptions, the change of the Pt−H distance in given complexes does not allow correlations between hydride shifts and metal−hydrogen bond length to be understood. Instead, variations in the polarization of metal 5d orbitals by the trans ligand affects the SO (and partly paramagnetic) shift contributions, as well as the Pt−H distances and the covalency of the metal−hydrogen bond (quantified, e.g., by natural atomic charges and delocalization indices from quantum theory atoms-in-molecules), resulting in a reasonable correlation of these structural/electronic quantities with hydride σ^{SO} shieldings. Our analysis also shows that specific σ^{P}- and σ^{SO}-active MOs are not equally important across the entire series. This explains some outliers in the correlation for limited ranges of trans-influence ligands. Additionally, SO effects from heavy-halide ligands may further complicate trends, indicating some limitations of the simple one-parameter correlations. Strikingly, σ-donating/π-accepting ligands with a very strong trans influence are shown to invert the sign of the usually shielding σ^{SO} contribution to the ^{1}H shifts, by a substantial reduction of the metal 5d orbital involvement in Pt−H bonding, and by involvement of metal 6p-type orbitals in the magnetic couplings, in violation of the Buckingham−Stephens "off-center ring-current" picture.

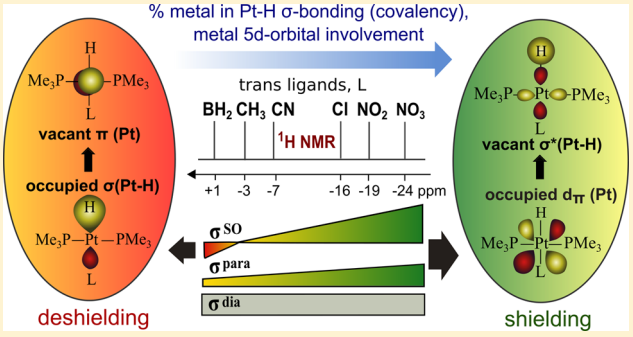

INTRODUCTION

The distinction between the trans influence as the ability of a ligand to weaken the metal−ligand bond trans to itself, which is thermodynamic in origin, and the kinetic trans effect on ligand substitution reactivity was introduced by Pidcock in 1960s.[1] Square-planar Pt(II) complexes have been studied most intensively in this context.[2] In addition to the bond length and binding energy of the trans metal−ligand bond, some spectroscopic parameters, such as vibrational frequencies, NMR chemical shifts, or nuclear spin−spin couplings, also tend to correlate with standard trans-influence series, and might thus serve as indicators. Chatt and Shaw showed some correlation between the trans-influence series and the ^{1}H NMR shifts for Pt(II) hydrides already in 1962.[3] For example, the hydride ligand has a more negative chemical shift when it is trans to a nitrate rather than a cyanide ligand. That is, a stronger trans donor ligand causes a less pronounced ^{1}H shielding. Buckingham and Stephens introduced an off-center ring-current model to explain the sometimes drastic low-frequency ^{1}H shifts of transition-metal hydride complexes.[4,5] They suggested that larger shielding should be caused mainly by a shorter M−H bond, related to the competition of the two trans ligands for the same sd-hybrid orbital of the metal center. Atkins et al. supported this assumption by reporting an almost linear correlation between ^{1}H NMR shifts and Pt−H IR stretching frequencies.[6] They excluded largely the ligand-field splitting (position of the trans ligand within the spectrochemical series) as a possible cause of the correlations. Birnbaum emphasized the position of the trans ligand in the nephelauxetic series and brought metal−ligand covalency into play.[7] The Buckingham−Stephens model was subsequently confirmed by density-functional theory (DFT) calculations.[8]

We have recently shown by fully relativistic DFT calculations of ^{1}H shifts in a wide variety of transition-metal hydride complexes that for 4d and in particular for 5d complexes spin−

Received: March 6, 2015

DOI: 10.1021/acs.inorgchem.5b00446
Inorg. Chem. XXXX, XXX, XXX−XXX

Table 1. Quasi-Relativistically Optimized Pt−H Distances, QTAIM Delocalization Indices (DI), NPA Atomic Charges (q) at the Hydride Ligand and Compositions (in %) of the Pt−H σ-Bonding NLMOs in *trans*-[HPtL(PMe_3)$_2$] Series along with Computed and Experimental ^{1}H NMR Hydride Shifts (in ppm vs TMS). The Spin−Orbit Part of the Isotropic Shielding (σ^{SO}) Is Given as well[a]

ligand	d(Pt−H)	DI(Pt↔H)	NPA	NLMO (Pt−H)			σ^{SO}(^{1}H)	δ_{calcd}(^{1}H)[b]	δ_{expt}(^{1}H)
L	[Å]		q(H)	%Pt	Pt(s)	Pt(d)	[ppm]	[ppm]	[ppm]
NO_3	1.548	1.004	−0.109	38.1	23.5	76.2	14.9	−23.6	−23.8[c]
ONO	1.562	0.990	−0.155	36.2	23.4	76.2	12.6	−20.1	−19.7[c,d]
Cl	1.565	0.987	−0.149	34.2	25.5	73.8	10.0	−15.8	−16.9[c]
Br	1.566	0.980	−0.147	33.8	25.5	73.8	9.6	−14.7	−15.6[c]
I	1.569	0.966	−0.149	32.7	25.4	73.8	8.3	−11.9	−12.7[c]
SCN	1.576	0.956	−0.156	32.2	23.5	76.0	7.8	−12.1	−13.3[c]
NO_2	1.582	0.968	−0.196	32.4	23.5	76.1	11.4	−19.0	−19.7[c,d]
CN	1.609	0.946	−0.251	26.6	24.7	74.8	3.1	−6.7	−7.8[c]
C_6H_5	1.628	0.923	−0.285	22.7	25.5	74.1	3.0	−5.9	−5.7[e]
CH_3	1.636	0.907	−0.305	20.8	23.7	75.4	1.2	−3.8	−3.8[e]
$Si(OMe)_3$	1.649	0.880	−0.328	15.5	23.6	75.1	−1.2	0.4	+0.7[f]
BCat	1.678	0.860	−0.377	13.1	30.6	68.3	−2.8	2.3	+0.4[g]

[a]See Computational Methods. [b]^{1}H NMR hydride shifts calculated at the 2c-ZORA(SO)/PBE0/TZ2P level including exchange-correlation kernel (cf. Figure 1 and Table S2 in Supporting Information for comparison of various computational methods). [c]Reference 3. The experimental values belong to *trans*-[HPtL(PEt_3)$_2$] measured in C_6D_6 (the τ values given in ref 3 were converted to the conventional NMR shift scale as $\delta = 10.0 - \tau$). [d]Doubtful assignment; see text. [e]Reference 43. The experimental values belong to *trans*-[HPtL(PPh_3)$_2$] measured in CD_2Cl_2. [f]Reference 44. The experimental value of *trans*-[HPt{Si(OMe)$_3$}(PEt_3)$_2$] in C_6D_6. [g]Reference 17a. The experimental value of *trans*-[HPt(BCat){P(CH_2Cy)$_3$}$_2$] in C_6D_6 (Cat = catecholate, 1,2-$O_2C_6H_4$).

orbit (SO) effects are important.[9] Note that in contrast to transition-metal complexes with a partially filled d-shell, d^0 and d^{10} hydrides, and even more so f^0 actinide hydrides, exhibit characteristic ^{1}H shifts in the very high-frequency range, and SO effects play a decisive role here as well.[10] The Buckingham−Stephens model thus must be augmented by sizable SO contributions, which may amount to roughly two-thirds of the observed low-frequency ^{1}H shifts in certain iridium and platinum hydride complexes.[9] In some of the analyzed systems, more negative ^{1}H shifts did not correlate well with larger ligand-field strength of the trans ligand, and it is thus desirable to revisit these correlations carefully. Here we apply quantitative relativistic DFT methodology to unravel the relations between electronic structure and ^{1}H shifts in transition-metal hydride complexes in much more detail than has hitherto been possible. In view of their general importance, particularly in catalysis, and of extensive previous studies, we focus our attention on square-planar Pt(II) d^8 hydride complexes.

COMPUTATIONAL METHODS AND THEORETICAL BACKGROUND

Gas-phase PBE0/def2-TZVP[11−13] (with quasi-relativistic, energy-adjusted small-core ECP for Pt and I)[14,15] structure optimizations were performed with the Turbomole program package.[16] The quality of the optimized structures was assessed by comparing salient bond lengths with X-ray structure data of some related square-planar platinum(II) hydride complexes[17] (cf. Table S1 in Supporting Information). Note that the popular B3LYP functional[18] provides noticeably longer bond lengths between the Pt center and non-hydrogen ligand atoms (by ∼0.05 Å), and it is thus not the best choice for this type of complex (cf. Table S1).

Quasi-relativistic DFT single-point calculations were performed using the Amsterdam density functional (ADF) program[19] at the generalized-gradient-approximation (GGA) level, using the Perdew−Burke−Ernzerhof (PBE) exchange-correlation functional,[11] as well as its one-parameter hybrid form (PBE0),[12] employing Slater-type orbital basis sets of triple-ζ doubly polarized (TZ2P)[20] quality and an integration accuracy parameter of 5.0. Relativistic effects were treated by the two-component (2c) zeroth-order regular approximation (ZORA)[21,22] to the Dirac equation, and gauge including atomic orbitals (GIAOs)[23] were used for the shielding calculations. The implementation of the ADF program used here includes the response of the first order exchange-correlation potential (xc kernel) for the calculated shielding implemented recently.[24]

Fully relativistic DFT calculations were performed at the four-component (4c) matrix Dirac−Kohn−Sham (mDKS) level of theory with the ReSpect program package.[25] The method combines GIAOs with restricted magnetically balanced (RMB) orbitals for the small component (this includes an xc kernel).[26,27] For comparison with the ADF results, the mDKS calculations were performed with the PBE functional as well. For the heavy atomic centers (Pt, Br, I), Dyall's all-electron valence-double-ζ (Dyall VDZ) basis sets[28] were employed. Fully uncontracted Huzinaga−Kutzelnigg-type IGLO-III basis sets[29] were used for the lighter ligand atoms ($Z < 18$). The calculated nuclear shieldings σ were converted to chemical shifts δ (in parts per million) relative to the shielding of tetramethylsilane (TMS) for ^{1}H and relative to *trans*-[HPtNO_3(PMe_3)$_2$] for ^{195}Pt, computed at the same level. These are also the reference standards used in the experiments we compare to.

Molecular orbital (MO) analyses of contributions to the shieldings were performed at two different levels: (a) using the analysis tools in the ADF code, both scalar relativistic and two-component ZORA results were broken down into MO (spinor) contributions; (b) additionally, one-component (1c) GIAO calculations of ^{1}H shieldings were done, based on combining Gaussian 09[30] to obtain the Kohn−Sham MOs and the local MAG property code[31] to compute both scalar-relativistic shifts and SO corrections. For the latter, Kohn−Sham orbitals with a Fermi-contact finite-perturbation at the nucleus of interest (finite-perturbation parameter $\lambda = 0.001$) were obtained, using the PBE functional, IGLO-III basis sets for the lighter ligand atoms, and Stuttgart relativistic small-core (RSC) effective core potentials (ECPs) with corresponding valence basis sets[14] for platinum and iodine. The perturbed MOs were transferred to MAG, which used RSC spin−orbit ECPs[32] to compute the SO corrections within the mixed finite perturbation approach of ref 33.

Analyses of atomic charges and of scalar relativistic natural localized molecular orbitals (NLMOs) were done with the NBO 5.0 module by Weinhold et al. in the ADF package.[34,35] Partially ionic natural-bond-orbital (NBO) Lewis structures with a lone pair on the hydride atom

DOI: 10.1021/acs.inorgchem.5b00446
Inorg. Chem. XXXX, XXX, XXX−XXX

were selected via the Choose keyword to invoke Lewis structures with equivalent phosphine ligands in the studied complexes with a C_{2v} symmetric *trans*-[$HPtP_2X$] core. NLMOs based on such a Lewis structure were analyzed. The lone pair NLMO on the hydride atom, with appreciable metal contribution, is denoted as BD(Pt−H). A corresponding shielding tensor analysis in terms of the full NLMO set was performed with the method reported in ref 36. Atomic contributions to the SO operators were obtained by selecting individual atomic contributions to individual ECP SO operators (for Pt, I, as well as an all-electron atomic-mean field SO operator for Br) in MAG. The delocalization index δ(A↔B), as a quantitative measure for the sharing of electrons in the context of the quantum theory of atoms-in-molecules (QTAIM),[37,38] was evaluated in the DGrid program[39] on the basis of single-point calculations performed with Gaussian09 using an all-electron Dyall VDZ basis set on Pt and def2-TZVP basis set on ligand atoms and employing a Douglas−Kroll−Hess second-order scalar relativistic Hamiltonian.[40] To distinguish this index from chemical shifts, we denote it as "DI" throughout this work. Bulk solvent effects on computed NMR shieldings were simulated via the conductor-like screening model (COSMO),[41] as implemented self-consistently in ADF.

RESULTS AND DISCUSSION

Correlation between Pt−H Distances and ^{1}H Chemical Shifts. The bond length in trans position to the considered ligand is often taken as a measure of the trans influence of a ligand.[42] As the precise position of the hydrogen atom near a heavy metal center is difficult to obtain experimentally, we may evaluate the correlation between Pt−H distances and ^{1}H shifts based on our optimized structures. In Table 1 the ligands were listed in the order of increasing Pt−H bond length, which is also the sequence of increasing trans influence, as found in many inorganic chemistry textbooks:

$$NO_3^- < ONO^- < Cl^- < Br^- < I^- < SCN^- < NO_2^- < CN^- < C_6H_5^- < CH_3^- < SiR_3^- < BR_2^-$$

The data confirm the well-known trend of a lengthening of the Pt−H bond with increasing σ-donor ability of the trans ligand, particularly for methanide, silanide, and boranide ligands.

The two- and four-component relativistic results for the ^{1}H hydride shifts of the same series of *trans*-[$HPtL(PMe_3)_2$] complexes are given in Table S2 in Supporting Information and are compared with experiment in Figure 1. Note that the experimental values sometimes belong to complexes with differently substituted phosphine ligands.[3,17,43,44] This may influence the hydride shifts but only moderately, as demonstrated for the *trans*-[$HPtCN(PR_3)_2$] series (R = H, Me, Et, Cy, Ph) in Table S3 in Supporting Information. Here, the largest difference is observed between complexes with PPh_3 and PCy_3 ligands (with $\delta(^1H)$ = −6.3 ppm and −7.6 ppm, respectively), while hydride shifts in Pt(II) complexes with methyl- and ethyl-substituted phosphine ligands differ only by 0.2 ppm. The generally somewhat more shielded hydride shifts for the [$HPtL(PCy_3)_2$] series are also evident by comparing experimental data from Table 1 with those in ref 45.

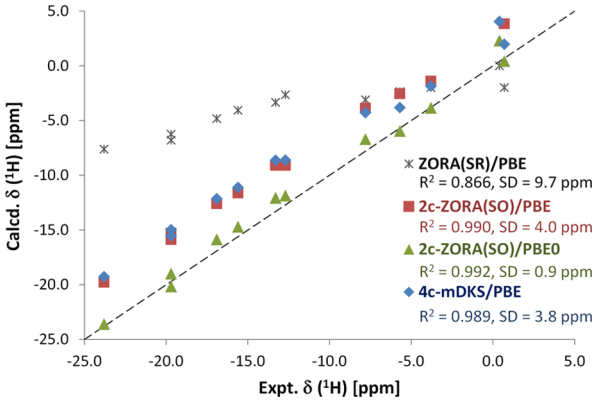

Figure 1. Computed vs experimental ^{1}H NMR hydride shifts (in ppm vs TMS) in *trans*-[$HPtL(PMe_3)_2$] complexes (cf. Table S2 in Supporting Information for numerical data). The dashed line represents the ideal agreement with experiment.

From Figure 1 it is particularly obvious that the scalar relativistic ZORA(SR) results for ^{1}H NMR hydride shifts tend to be insufficiently negative. In keeping with our previous findings,[9] this is improved significantly by inclusion of SO effects. The two-component relativistic ZORA(SO) (including SO coupling) and the four-component mDKS results with the PBE functional agree well with each other, and both reproduce the experimental trend in hydride shifts very well (R^2 > 0.98), although the computed shifts are systematically too deshielded by ∼3−4 ppm. Excellent agreement between theory and experiment (with R^2 = 0.992 and a standard deviation of 0.9 ppm) is achieved by using the 2c-ZORA(SO) method in conjunction with the hybrid PBE0 functional. This method is thus preferred in further discussion and analysis. Note that the current 4c-mDKS ReSpect implementation of chemical shifts does not yet allow for GIAO calculations with hybrid functionals, and it is under development. Furthermore, it is clear that inclusion of the kernel in the modified ADF implementation[24] is important for good agreement. Table S2 in Supporting Information demonstrates that the previous 2c-ZORA implementation of nuclear shieldings in ADF without kernel provides insufficiently negative ^{1}H shifts, particularly for systems with larger σ^{SO} contribution (with a maximum deviation of 4.4 ppm from experiment for the nitrato complex when using the PBE0 functional). Indeed, if we delete the kernel contributions in the 4c-mDKS ReSpect calculations, we see the same deterioration (see the PBE results in Table S2). Inclusion of bulk solvent effects by the COSMO solvation model (assuming benzene and CH_2Cl_2 as solvent, respectively) leads to only a marginal improvement of computed hydride shifts, reducing the standard deviation by 0.1 ppm (Table S4 in Supporting Information).

Figure 2 shows that more negative ^{1}H shifts are indeed roughly correlated to shorter Pt−H bonds, as emphasized early on by Buckingham and Stephens.[4] A trans influence series for the ^{1}H hydride shifts is

$$NO_3^- < ONO^- < NO_2^- < Cl^- < Br^- < SCN^- \approx I^- < CN^- < Ph^- < Me^- < SiR_3^- \approx BR_2^-$$

The N-nitrito complex at first sight provides the clearest outlier, as had been noted already by Chatt and Shaw.[3] The measured and computed proton shift is at less negative value than expected from the usual trans effect series. It had been suggested that the nitrito group is actually bound to platinum by one of its oxygen atoms. However, our computations show that this would affect the hydride shift only marginally—the O-nitrito complex exhibits a very similar computed value (cf. Table 1). Moreover, measured spin−spin coupling constants later confirmed an N-nitrito complex.[46]

While the N-nitrito complex with its "too negative" shift is the most apparent outlier, the halide complexes deviate in the

DOI: 10.1021/acs.inorgchem.5b00446
Inorg. Chem. XXXX, XXX, XXX−XXX

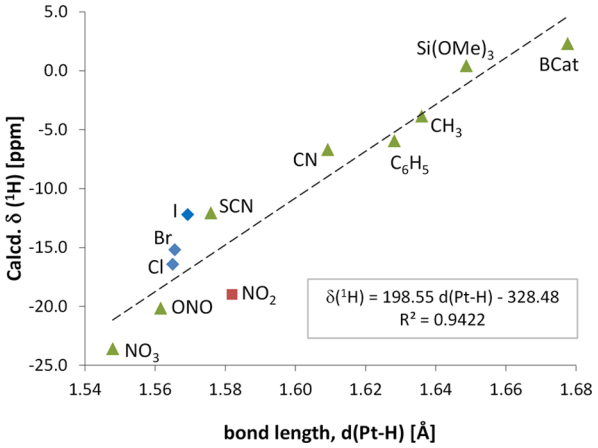

Figure 2. Correlation between computed ^{1}H NMR hydride shifts (2c-ZORA(SO)/PBE0/TZ2P results) and optimized Pt−H bond lengths in *trans*-[HPtL(PMe$_3$)$_2$] series (cf. Table 1). The dashed line represents the linear-regression line of the values represented by triangles.

positive direction (cf. Figure 2 and discussion below). The nitrite ligand is in any case an example that shows previous interpretations to be incomplete: while the N- and O-nitrito compounds exhibit very similar ^{1}H shifts, the N-nitrito complex clearly has a longer Pt−H bond (cf. Table 1). On the other hand, the N-nitrito and S-thiocyanato complexes exhibit similar Pt−H distances but rather different hydride shifts. These cases indicate that a rationalization of the shifts via the Pt−H distances does not cover all aspects of the problem. A more detailed theoretical analysis is thus desirable.

Shielding-Tensor Contributions. We separate the shielding (both isotropic value and tensor components) into the well-known diamagnetic (σ^d) and paramagnetic (σ^p) terms and into a spin−orbit (σ^{SO}) term. Table 2 shows such a breakdown obtained at the 2c-ZORA-GIAO-PBE0/TZ2P level. We note that the separation into σ^d and σ^p is not unique but depends on the chosen gauge of the magnetic vector potential. Here we followed the previous convention for definition of diamagnetic and paramagnetic terms at DFT-GIAO level by Ziegler and co-workers.[22,47] Separation of the SO terms also follows the standard procedure for the 2c-ZORA-GIAO-PBE0/TZ2P level.[48]

We see that the isotropic σ^d remains almost constant (within less than 2.2 ppm) across the series of trans ligands. This constancy is usually assumed for all nuclei except hydrogen (or helium). For proton shifts it is not self-evident, as hydrogen has no (spherical) core−shell, and we show below that the diamagnetic contribution to the shielding tensor is in fact highly anisotropic. Nevertheless, for the purpose of analyzing the trans influence on the isotropic ^{1}H hydride shifts, we may concentrate on σ^p and σ^{SO} (Figure 3).

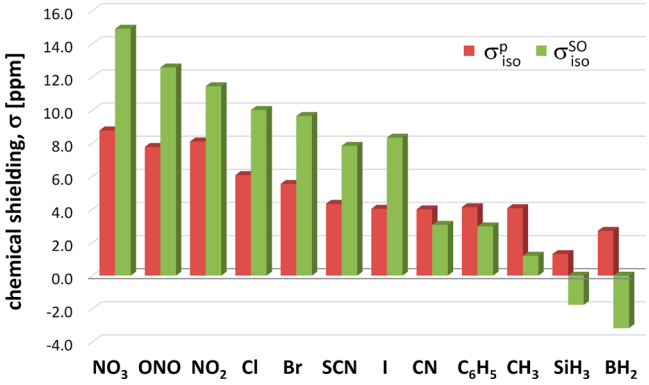

Figure 3. Dependence of the computed paramagnetic and SO contributions to isotropic hydride ^{1}H shielding on trans ligand L in the [HPtL(PMe$_3$)$_2$] series (2c-ZORA(SO)/PBE0/TZ2P results; cf. Table 2 and Table S5 for numerical data).

Across the entire series, the isotropic σ^p varies by up to 7.5 ppm, σ^{SO} by ∼18 ppm! Furthermore, the σ^d and σ^p contributions alone explain neither the large low-frequency hydride shifts for complexes involving ligands with weak trans influence nor the positive ^{1}H shift values recorded for some silyl and boryl complexes. It is thus clear that σ^{SO} dominates the dependence of the shielding on the trans ligand. While the σ^p and σ^{SO} trends go roughly parallel for "weak" trans ligands (suggesting related electronic-structure origins), notable differences between the two terms are seen for strong σ-donor ligands. For example, we see that the isotropic σ^p remains relatively unchanged for the ligands SCN$^-$, CN$^-$, CH$_3^-$, and BH$_2^-$ (within less than 1.5 ppm), whereas σ^{SO} still drops significantly along the same series and changes from positive to negative sign for the strongest σ-donors (Figure 3).

In addition, bromine and particularly iodine are both sufficiently heavy to contribute noticeably to the SO effects on the ^{1}H shifts.[49] Analyses at the one-component perturbational level (by removing individual SO-ECPs) show contributions of −0.3 ppm for Br and of −1.3 ppm for I to the ^{1}H shieldings. Converted into shifts, halogen SO contributions hence provide an explanation for the "too positive" shifts in Figure 2 for L = Br, I.

Table 2. Calculated Components of the Hydride ^{1}H Shielding Tensors (in ppm) in Selected *trans*-[HPtL(PMe$_3$)$_2$] Complexes and Their Separation into Diamagnetic (σ^d), Paramagnetic (σ^p) and Spin−Orbit (σ^{SO}) Terms[a]

L	$\sigma^d_{\parallel}$	$\sigma^d_{\perp,ip}$	$\sigma^d_{\perp,op}$	σ^d_{iso}	$\sigma^p_{\parallel}$	$\sigma^p_{\perp,ip}$	$\sigma^p_{\perp,op}$	σ^p_{iso}	$\sigma^{SO}_{\parallel}$	$\sigma^{SO}_{\perp,ip}$	$\sigma^{SO}_{\perp,op}$	σ^{SO}_{iso}
NO_3	58.7	23.7	12.2	31.5	−4.9	13.1	18.1	8.8	−2.2	22.2	24.7	14.9
Cl	58.2	23.1	12.7	31.3	−3.8	7.5	14.5	6.1	−2.1	14.2	17.9	10.0
NO_2	57.0	23.4	12.8	31.1	−5.0	12.2	17.1	8.1	−2.5	15.4	21.4	11.4
CN	55.9	23.6	14.0	31.2	−3.7	5.2	10.5	4.0	−3.0	0.3	11.9	3.1
CH_3	54.1	23.2	13.0	30.1	−2.7	4.4	10.5	4.1	−3.6	−2.9	10.1	1.2
SiH_3	53.8	23.2	13.3	30.1	−4.4	0.7	7.6	1.3	−3.8	−11.1	9.6	−1.8
BH_2	51.2	23.1	13.7	29.3	−6.1	0.2	14.0	2.7	−5.0	−17.8	13.3	−3.2

[a]2c-ZORA(SO)/PBE0/TZ2P results; isotropic shielding $\sigma_{iso} = \sigma^d_{iso} + \sigma^p_{iso} + \sigma^{SO}_{iso}$, where $\sigma^k_{iso} = (\sigma^k_{\parallel} + \sigma^k_{\perp,ip} + \sigma^k_{\perp,op})/3$ (k = d, p, SO). Data for all Pt(II) hydride complexes are given in Table S5 in Supporting Information. Model complexes with SiH_3 and BH_2 trans ligands possess similar hydride shifts as their Si(OMe)$_3$ and BCat congeners and are therefore used in further analysis.

DOI: 10.1021/acs.inorgchem.5b00446
Inorg. Chem. XXXX, XXX, XXX−XXX

Molecular Orbital Analysis of σ^p. While σ^{SO} dominates the overall trends, we start our closer MO analysis with σ^p for a number of complexes (at the scalar-relativistic ZORA level). For closer analysis it is important to distinguish the individual components of the $\boldsymbol{\sigma}^p$ tensor, which is clearly anisotropic (cf. Table 2). That is, we obtain $\sigma^p_{\parallel}$ parallel to the Pt−H bond, $\sigma^p_{\perp,ip}$ perpendicular to the Pt−H bond but in the plane of the complex, and the out-of-plane perpendicular component, $\sigma^p_{\perp,op}$ (cf. Figure 4). As predicted by the Buckingham−Stephens model,[4] it is the two perpendicular components that provide an overall shielding contribution, while the parallel component is deshielding. This had been confirmed by DFT calculations, which, however, gave much lower shielding anisotropies than the original Buckingham−Stephens model predictions.[8]

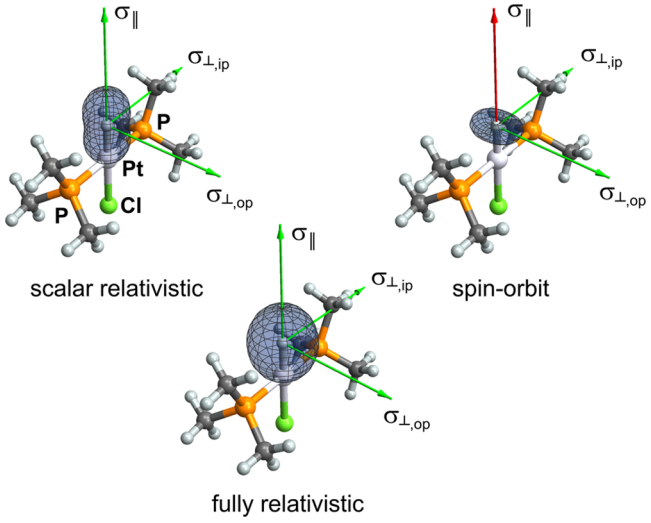

Figure 4. Scalar-relativistic ($\boldsymbol{\sigma}^d + \boldsymbol{\sigma}^p$), spin−orbit ($\boldsymbol{\sigma}^{SO}$), and fully relativistic hydride shielding tensors in *trans*-[HPtCl(PMe$_3$)$_2$], represented as polar plots of functions^{S0} $\sum_{ij} r_i r_j \sigma_{ij}$ (a green arrow indicates a shielding contribution; a red one indicates a deshielding contribution).

The comparison in Table 2 reveals (a) very anisotropic but closely similar diamagnetic shielding tensors for all complexes; (b) the main changes of the isotropic σ^p are clearly due to the two perpendicular paramagnetic shielding tensor contributions (e.g., $\sigma^p_{\perp,ip}$ decreases by ∼13 ppm with increasing trans influence), whereas the parallel contributions differ much less ($\sigma^p_{\parallel}$ changes overall by ca. 3.5 ppm).

To what extent are changes in the Pt−H distance the direct *cause* of the trends in paramagnetic shieldings, as implied by previous studies?[S1] This is probed in Table 3 for the chloro and cyano complexes as examples, by contracting or expanding, respectively, the Pt−H distance by 0.05 Å from its optimized value. We first of all note that the overall changes in shielding tensor components (and isotropic values as well) upon elongation/shortening of Pt−H bonds are significantly less than the range covered by complexes with different trans ligands (cf. Tables 2 and 3), although they show a comparable range of Pt−H distances [cf. d(Pt−H) values in Tables 1 and 3]. That is, the direct distance dependence of the perpendicular paramagnetic shieldings is quite small and does not support the original interpretations by Buckingham and Stephens.[4]

The main trans effects on σ^p arise from the perpendicular components (Table 2). We separate these components into contributions from individual couplings between occupied and virtual canonical MOs obtained from scalar relativistic ZORA-GIAO calculations. We focus here on the comparison between the CN and BH$_2$ complexes as examples with strong trans influence and small σ^p values, on the Cl complex with a medium trans influence, and on the NO$_3$ complex as a case with weak trans influence and large shielding contributions. The analysis shows that σ^p values arise from numerous contributions, but there are only a few that stand out by being larger and by differing more between the complexes (cf. Table 4; the main MOs contributing to σ^p and σ^{SO} are shown in Figure 5).

In agreement with the Buckingham−Stephens model[4] and previous DFT analyses,[8] these contributions are mainly caused by couplings between (in-plane and out-of-plane) d_π-type occupied MOs and the σ^*(Pt−H)-type unoccupied MO(s) with some d-metal character and s orbital contribution from the hydride atom (cf. Figure 5). While coupling of the in-plane d_π-type MO to the σ^*(Pt−H)-type MO dominates the out-of-plane perpendicular component of $\boldsymbol{\sigma}^p$, the out-of-plane d_π-type MO contributes to the in-plane perpendicular component. These contributions are significantly larger for the NO$_3$ than for the CN and BH$_2$ complexes, thus also explaining differences in the isotropic σ^p contributions for these systems.

Analogous dominant occupied-virtual MO couplings, which originate from in-plane or out-of-plane d_π-type MOs, are found to be largely responsible also for the trans ligand influences on σ^p of the other complexes (see Table S8 and Figure S1 in Supporting Information for analyses on more complexes). Overall, these few contributions from d_π-type MOs reflect the entire σ^p trend in the trans influence series.

MO Analysis of σ^{SO}. We showed above that the trans influence is largely dictated by σ^{SO}. Table 2 shows that the two perpendicular components of $\boldsymbol{\sigma}^{SO}$ are responsible for the important SO shielding (as well as for the small SO deshielding in the case of silyl and boryl complexes), and these components are both significantly smaller for ligands with strong trans influence than for weak trans-influence ones. The trends for the

Table 3. Computed Hydride ^{1}H NMR Shielding Tensor Components (in ppm) in *trans*-[HPtL(PMe$_3$)$_2$] (L = Cl, CN) Complexes as a Function of Pt−H Distance[a]

L	d(Pt−H)[Å]	$\sigma^d_{\parallel}$	$\sigma^d_{\perp,ip}$	$\sigma^d_{\perp,op}$	σ^d_{iso}	$\sigma^p_{\parallel}$	$\sigma^p_{\perp,ip}$	$\sigma^p_{\perp,op}$	σ^p_{iso}	$\sigma^{SO}_{\parallel}$	$\sigma^{SO}_{\perp,ip}$	$\sigma^{SO}_{\perp,op}$	σ^{SO}_{iso}
Cl	1.505	61.5	23.7	13.0	32.7	−4.2	7.5	15.2	6.2	−2.0	13.4	16.2	9.2
	1.565	58.2	23.1	12.7	31.3	−3.8	7.5	14.5	6.1	−2.1	14.2	17.9	10.0
	1.605	55.2	22.6	12.6	30.1	−3.5	7.4	13.9	5.9	−2.2	15.2	19.8	10.9
CN	1.559	59.0	24.1	14.2	32.4	−4.0	5.2	11.1	4.1	−2.9	0.4	10.7	2.7
	1.609	55.9	23.6	14.0	31.2	−3.7	5.2	10.5	4.0	−3.0	0.3	11.9	3.1
	1.659	53.2	23.2	13.9	30.1	−3.4	5.2	10.0	3.9	−3.0	0.2	13.2	3.5

[a]2c-ZORA(SO)/PBE0/TZ2P results (cf. Computational Methods and footnotes in Table 2).

DOI: 10.1021/acs.inorgchem.5b00446
Inorg. Chem. XXXX, XXX, XXX−XXX

Table 4. Selected Contributions from Occupied MOs with d_π Character to the Paramagnetic Part of the ^{1}H NMR Hydride Shielding Tensor, σ^p, in Pertinent *trans*-[HPtL(PMe$_3$)$_2$] Complexes[a]

L	molecular orbitals	σ^p_{iso} [ppm]	$\sigma^p_{\parallel}$ [ppm]	$\sigma^p_{\perp,ip}$ [ppm]	$\sigma^p_{\perp,op}$ [ppm]	ΔE [eV]
NO_3	HOMO−2	3.2	−0.7	10.2	0.0	
	(HOMO−2→LUMO+1)	(2.0)	(0.0)	(6.0)	(0.0)	6.80
	HOMO−3	3.0	−0.5	0.4	9.0	
	(HOMO−3→LUMO+1)	(1.2)	(0.0)	(0.0)	(3.6)	7.25
	HOMO−6	1.6	−1.4	−0.6	6.8	
	(HOMO−6→LUMO+1)	(1.9)	(0.0)	(0.0)	(5.6)	8.03
Cl	HOMO	1.4	−0.1	4.0	0.0	
	(HOMO→LUMO+1)	(0.6)	(0.0)	(1.8)	(0.0)	6.41
	HOMO−2	2.1	0.0	0.4	5.9	
	(HOMO−2→LUMO+1)	(1.0)	(0.0)	(0.0)	(3.0)	6.61
	HOMO−6	1.2	−0.3	4.2	−0.4	
	(HOMO−6→LUMO+1)	(1.0)	(0.0)	(3.0)	(0.0)	8.10
	HOMO−7	1.6	−0.7	−0.2	5.7	
	(HOMO−7→LUMO+1)	(1.8)	(0.0)	(0.0)	(5.5)	8.57
CN	HOMO−1	1.4	−0.2	4.4	0.0	
	(HOMO−1→LUMO+2)	(0.5)	(0.0)	(1.5)	(0.0)	7.37
	HOMO−2	2.2	0.0	0.3	6.2	
	(HOMO−2→LUMO+2)	(1.0)	(0.0)	(0.1)	(2.9)	7.65
BH_2	HOMO−5	1.1	0.5	1.0	1.7	
	(HOMO−5→LUMO+4)	(0.4)	(0.2)	(0.4)	(0.6)	8.65

[a]Individual contributions from couplings of the given occupied MOs to σ^*(Pt−H) virtual MOs are given in parentheses. ZORA(SR)/PBE0/TZ2P results. See Figure 5 for plots of the relevant MOs.

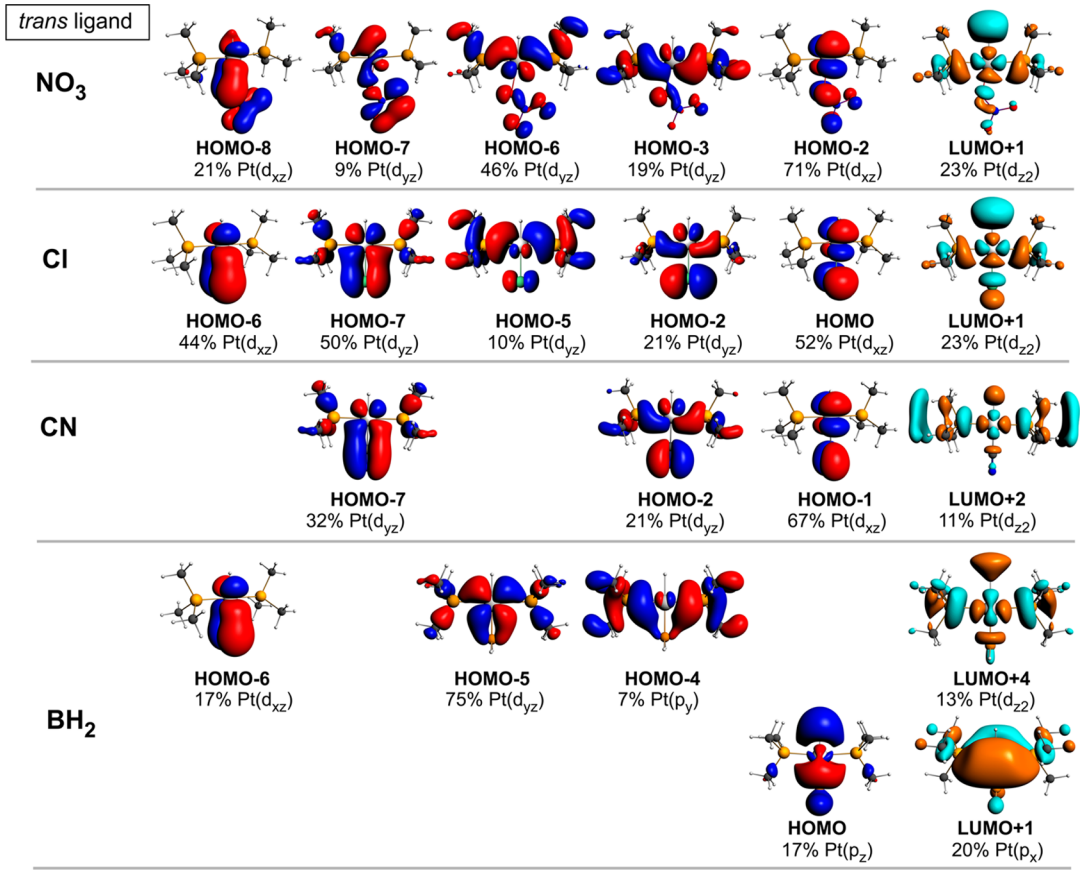

Figure 5. Isosurface plots (±0.03 au) of the dominant occupied and virtual MOs contributing to the $\boldsymbol{\sigma}^p$ and $\boldsymbol{\sigma}^{SO}$ tensors in selected *trans*-[HPtL(PMe$_3$)$_2$] complexes (cf. Tables 4 and 5). Contributions from the Pt d-orbitals (and p-orbitals where applicable) in percent are indicated. The symmetry of the dominant Pt(5d)/Pt(6p) atomic orbitals is indicated in parentheses (*z* corresponds to a twofold rotation axis along the Pt−H bond; *y* and *x* axes lie in-plane and out-of-plane, respectively).

DOI: 10.1021/acs.inorgchem.5b00446
Inorg. Chem. XXXX, XXX, XXX−XXX

out-of-plane component go roughly parallel to the two perpendicular components of $\boldsymbol{\sigma}^{p}$ (Table 2), whereas the trend for the in-plane component of $\boldsymbol{\sigma}^{SO}$ is more pronounced. This indicates that the SO shieldings in these hydride complexes may be viewed as an extension of the Buckingham−Stephens model,[9] but with some modifications (see below). The SO contributions in Table 3 show, furthermore, that there is almost no direct distance dependence of these contributions. This may be attributed to the almost constant metal 5d-orbital involvement in the Pt−H bonds upon their elongation/shortening when keeping the trans ligand unchanged. That is, the correlation between measured shieldings and Pt−H distances has an indirect rather than direct origin also for the SO contributions (see above). In fact, the shorter Pt−H bond length provides even the smaller isotropic σ^{SO} shielding contribution, although only by a small margin (cf. Table 3).

Note that due to the large anisotropy of $\boldsymbol{\sigma}^{d}$ compared to $\boldsymbol{\sigma}^{p}$ (with a dominant parallel $\sigma_{\parallel}^{d}$ component), the "scalar relativistic" hydride shielding tensor ($\boldsymbol{\sigma}^{d} + \boldsymbol{\sigma}^{p}$) has its largest shielding component along the Pt−H bond. The SO-induced shielding ($\boldsymbol{\sigma}^{SO}$), which contributes predominantly to the two perpendicular components, makes the "fully relativistic" shielding tensor less anisotropic in most cases (cf. Figure 4 and Table S6 in Supporting Information). This contrasts, for example, to some five-coordinate square-pyramidal Ir(III) and Rh(III) complexes, where SO effects give rise to highly anisotropic shielding tensors.[9] The predicted anisotropies in the latter systems have very recently been confirmed by solid-state $^{1}H/^{2}H$ NMR experiments.[52]

MO analyses of the SO contributions may be obtained by subtraction of MO contributions obtained in scalar-relativistic calculations from the corresponding MO (spinor) contributions of two-component ZORA-SO calculations. Table 5 shows

Table 5. Dominant Occupied-MO Contributions to the Spin-Orbit Part of the ^{1}H NMR Hydride Shielding Tensor, $\boldsymbol{\sigma}^{SO}$, in Pertinent *trans*-[HPtL(PMe$_3$)$_2$] Complexes[a]

ligand L	MO contributions	σ_{iso}^{SO} [ppm]	$\sigma_{\parallel}^{SO}$ [ppm]	$\sigma_{\perp,ip}^{SO}$ [ppm]	$\sigma_{\perp,op}^{SO}$ [ppm]
NO_3	HOMO−3 (→LUMO+1)	3.1	−0.9	1.0	9.3
	HOMO−6 (→LUMO+1)	2.3	−1.1	−1.2	9.2
	HOMO−7 (→LUMO+1)	2.3	−0.2	1.8	5.3
	HOMO−8 (→LUMO+1)	5.8	0.4	17.4	−0.5
Cl	HOMO−5 (→LUMO+1)	6.2	−0.1	2.2	16.5
	HOMO−7 (→LUMO+1)	3.5	−0.9	1.3	10.2
CN	HOMO−7 (→LUMO+2)	4.0	−0.7	1.0	11.7
BH_2	HOMO (→LUMO+1)	−7.2	−9.5	−7.4	−4.7
	HOMO−4 (→LUMO+4)	2.1	0.9	2.0	3.5
	HOMO−5 (→LUMO+4)	1.7	0.2	1.5	3.4
	HOMO−6 (→LUMO+4)	1.4	2.6	1.4	0.1

[a]2c-ZORA(SO)/PBE0/TZ2P results (cf. Computational Methods). The dominant occupied-virtual MO couplings are indicated in parentheses.

the dominant contributions to the $\boldsymbol{\sigma}^{SO}$ tensor, which stem in most cases from coupling between the occupied in-plane and out-of-plane d_π-type and virtual σ^*(Pt−H) MOs (note that σ and π-type symmetry is given here with respect to the Pt−H bond). Although the platinum d_π-type MO contributions reflect the overall trend when considering only ligands with weak and medium trans influence, the dominant contributors to σ^{p} are not equally important for σ^{SO} (cf. Table S7 in Supporting Information). Note also that other couplings contribute to σ^{SO} as well, in particular, for the strongest σ-donors (L = alkyl, SiR_3, BR_2). Here, magnetic couplings from occupied σ(Pt−H)-type MOs into vacant π-type MOs (both involving platinum 6p orbitals) come into play and are responsible for the deshielding (negative σ^{SO}) contribution, which counteracts the shielding SO effect from $5d_\pi \rightarrow 5d_\sigma$*-based couplings (cf. Table 5 and Table S9 in Supporting Information for more data). Now the magnitude and the sign of the hydride σ^{SO} is based on a balance between various shielding (predominantly $5d_\pi \rightarrow 5d_\sigma$*) and deshielding ($5d/6p_\sigma \rightarrow 6p_\pi$) magnetic couplings. This results, for example, in a substantial reduction of σ^{SO} for *trans*-[HPtMe(PMe$_3$)$_2$] (still with slightly predominant d_π(Pt) → σ^*(Pt−H) transitions) and in a change to negative σ^{SO} for silyl and boryl complexes (with a dominant deshielding contribution from the magnetic coupling between the σ-type highest occupied molecular orbital (HOMO), with appreciable Pt($6p_z$) character and the vacant π-type second lowest unoccupied molecular orbital (LUMO+1) with 20% Pt($6p_x$) character).

In Supporting Information, we also provide an analysis of SO shieldings obtained at one-component perturbation level based on a scalar relativistic calculation (see Tables S15 and S16 and Figure S2), which gives a qualitatively similar MO picture.

Recently, Vicha et al.[53] have studied the influence of electronic and structural effects on the σ^{SO} contributions to ^{15}N NMR shifts for a series of d^6 iridium complexes by stretching trans bonds and modifying trans ligands. They found correlations with the nitrogen s-orbital character of the Ir−N bond, with energy gaps and, most importantly, with the iridium d-orbital character in the Ir−N bond. Notably, these authors argued not only via the FC matrix elements, as is often done,[54,55] but emphasized the SO matrix elements as decisive. Consistent with the present work, those authors also recognized the shielding and deshielding SO contributions coming from 5d → 5d* and 6p → 6p* magnetic couplings, respectively, on ^{13}C and ^{15}N NMR shifts in some 2-phenylpyridine d^8 complexes of platinum(II) and gold(III).[56] We show here additionally, that a deshielding SO effect due to $6p_\sigma \rightarrow 6p_\pi$-based magnetic couplings may be induced in Pt(II) complexes by introducing ligands with a strong trans influence, without changing the transition-metal center (Pt(II) → Au(III) in ref 56).

As the hydrogen s-orbital character in the Pt−H bond (relevant for the Fermi-contact interaction) is largely constant within the present series, it is the SO coupling of platinum 5d orbitals that dominates the hydride σ^{SO}. It is thus to be expected that the trans ligand influence on σ^{SO} may indeed reflect the metal d-orbital contributions to the relevant MOs. Using the relativistic NMR shielding analysis method based on NLMOs,[36] it can be shown that the percentage of Pt character (and thus the metal d-orbital involvement) in the Pt−H bond goes parallel with the σ^{SO} contribution due to this NLMO, which causes almost the entire σ^{SO} term (cf. Table S11 in Supporting Information). Together, these observations suggest that the more covalently bound ligands with strong trans influence polarize the relevant Pt(5d) atomic orbitals away from the Pt−H bond, which is accompanied by a decrease of the Pt−H bond covalency (cf. NPA atomic charges and QTAIM delocalization indices in Table 1). Such ligands thus diminish the relevant matrix elements, both for σ^{SO} and σ^{p}. This is demonstrated in Figure 6, which shows a very good correlation of the hydride σ^{SO} term with the metal percentage contribution to the Pt−H σ-bonding NLMO as well as with the

DOI: 10.1021/acs.inorgchem.5b00446
Inorg. Chem. XXXX, XXX, XXX−XXX

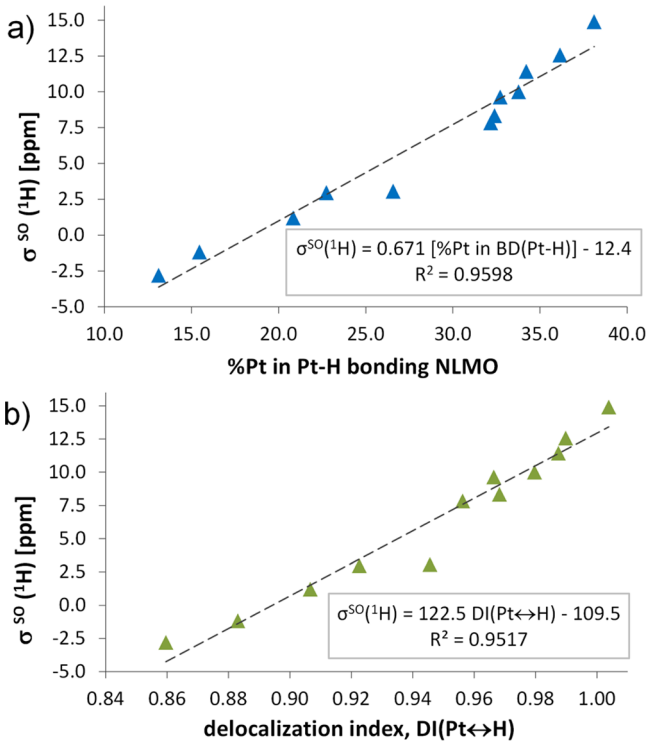

Figure 6. Correlation of the SO-induced isotropic hydride shielding σ^{SO} with a) the percentage of metal character in the Pt−H σ-bonding NLMO and b) the QTAIM delocalization index.

QTAIM delocalization index DI(Pt↔H), as a measure of the covalency of the Pt−H bond.

Somewhat poorer but still reasonable linear plots are also found for correlations of σ^{SO} with the optimized Pt−H bond lengths (R^2 = 0.9148) and with the hydride atomic charges (R^2 = 0.9443; see Figures S3 and S4 in Supporting Information).

Correlation between ^{1}H and ^{195}Pt NMR Shifts. The Buckingham−Stephens off-center ring-current model[4] would suggest that the same paratropic ring currents within the incomplete metal d-shell will lead to a deshielding of the metal nucleus and the well-known shielding of the hydride proton. Indeed, already in 1968 Dean and Green found a moderately good correlation between ^{195}Pt and ^{1}H NMR chemical shifts for a series of platinum hydride complexes.[51] Deviations from ideal correlation were attributed to the dependence of the ^{1}H shifts on the Pt−H distance (see above), in contrast to the ^{195}Pt shifts, which should be affected less.

The above results for the proton shifts suggest a different interpretation for the incomplete correlation: the hydride ^{1}H shifts are to a large extent determined by the SO shifts arising from platinum SO coupling. This is often termed a heavy-atom effect on the light atom shielding (HALA effect).[54,55] In contrast, platinum SO effects on the ^{195}Pt shieldings belong to the heavy-atom effects on the heavy-atom shielding (HAHA effects), which were shown to be essentially atomic in nature and to thus largely cancel for relative shift trends.[57−59] The ^{195}Pt shift trends are thus expected to be dominated by the σ^p term,[60] unless heavy atoms are bonded to platinum, which could give rise to HALA SO effects. The latter should apply only to the halide ligands.

We thus computed also the ^{195}Pt shifts, both at 2c-ZORA-SO and at 4c-mDKS levels (Table 6). Note again that the experimental values are for compounds with ethyl-substituted phosphine ligands, while we compute the methyl-substituted complexes for consistency with the ^{1}H chemical shifts. Both methods give closely comparable relative shifts, even though larger differences are observed for absolute ^{195}Pt shieldings (cf. Tables S12 and S13 in Supporting Information). The effect of the substituents on the ^{195}Pt shifts is more pronounced than for the ^{1}H hydride shifts, in particular when replacing trialkylphosphine ligands for aryl analogues (cf. Table S3 in Supporting Information), but it is anticipated to have a marginal impact on relative shift trends. The calculated ^{195}Pt chemical shifts at 2c-ZORA-SO as well as at 4c-mDKS levels agree very well with experiment, given the known sensitivity of ^{195}Pt shifts to a variety of factors, including solvent effects.[61,62] Note that the bulk solvent effects on ^{195}Pt NMR shifts simulated by the COSMO solvation model are only marginal (cf. Table S14 in Supporting Information), but some specific interactions (such as a coordination of solvent molecules) may play a role as well.

Figure 7 plots the obtained ^{1}H hydride shifts against the ^{195}Pt data. A good inverse correlation (lower proton shifts with larger platinum shifts) is found only for the Pt(II) complexes, where L = NO_3, ONO, SCN, CN (green triangles), and for the chloro complex. The bromo and iodo complexes deviate considerably from the correlation line, due to the large negative halogen HALA SO contributions to the platinum shift, in particular of course for the iodo complex. Indeed, if we artificially switch off

Table 6. Calculated and Experimental ^{195}Pt NMR Shifts in the *trans*-[HPtL(PMe_3)$_2$] Series[a]

ligand L	δ^{Pt}_{2c} (PBE) [ppm]	δ^{Pt}_{4c} (PBE) [ppm]	δ^{Pt}_{2c} (PBE0) [ppm]	expt[b] [ppm]
NO_3	0.0	0.0	0.0	0.0
ONO	43.2	57.3	8.9	−60.3
Cl	−161.2	−163.7	−168.5	−137.4
Br	−250.7	−273.0	−267.6	−249.3
I	−421.7	−443.7	−452.5	−442.9
SCN	−200.3	−184.9	−262.9	−248.9
CN	−268.8	−239.6	−362.0	−408.3

[a]NMR shifts in parts per million vs *trans*-[HPtNO$_3$(PMe_3)$_2$] as the primary reference standard. δ^{Pt}_{2c}: 2c-ZORA(SO) results with TZ2P basis set; δ^{Pt}_{4c}: 4c-mDKS results using a Dyall VDZ/IGLO III basis set (cf. Computational Methods). [b]Reference 51. The experimental values for *trans*-[HPtL(PEt_3)$_2$] were measured in acetone-d_6.

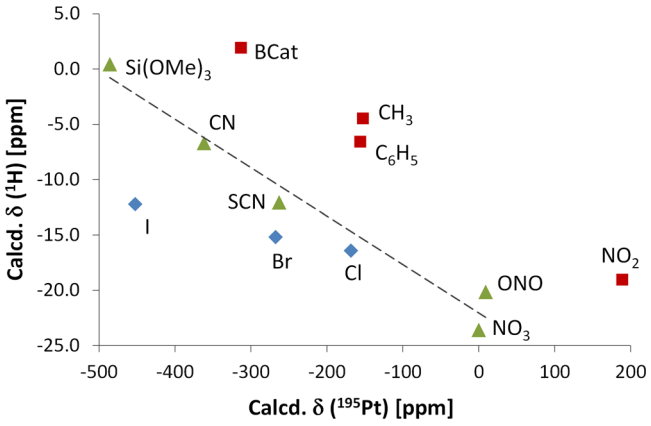

Figure 7. Correlation of computed ^{1}H and ^{195}Pt chemical shifts within the *trans*-[HPtL(PMe_3)$_2$] series (2c-ZORA(SO)/PBE0/TZ2P results). See data in Tables 1 and 6. The dashed line represents the linear-regression line of the values represented by green triangles.

DOI: 10.1021/acs.inorgchem.5b00446
Inorg. Chem. XXXX, XXX, XXX−XXX

the halogen contributions, the points for the bromo and iodo complex fall closer to the correlation line (data not shown).

Including also computed shifts for the other trans platinum hydrides (L = NO_2, C_6H_5, CH_3, $Si(OMe_3)_3$, BCat), where no experimental ^{195}Pt values are available, provides still much poorer correlation with the hydride shifts (Figure 7). This is most striking for the N-nitrito complex, which exhibits a comparably more deshielded ^{195}Pt signal, whereas the other Pt(II) complexes are shielded relative to *trans*-$[HPtNO_3(PMe_3)_2]$. Indeed, the very limited correlation between the shifts of the two nuclei should not be too surprising, given the various SO and non-SO contributions we have identified, in particular, for the proton shifts.

CONCLUSIONS

We have recently demonstrated the often appreciable importance of SO effects for the strikingly negative ^{1}H shifts of heavy transition-metal hydride complexes with d^6 or d^8 configurations.[9] This observation has prompted the present study, which has revisited the long-appreciated correlations of these ^{1}H hydride shifts with the trans ligand influence series, with Pt−H distances, and with ^{195}Pt shifts in a series of square-planar Pt(II) complexes.

We find that the paramagnetic and SO shielding contributions go roughly in parallel for "weak" and "medium" trans ligands and tend to be dominated by magnetic couplings between the d_π-type occupied and σ^*(Pt−H) virtual MOs. In general, it is, however, the SO shifts that dominate the observed trans ligand dependencies. The correlations between σ^p and σ^{SO} may break down, for example, due to SO effects arising from heavy halide substituents or due to additional magnetic couplings between occupied σ(Pt−H) and vacant π-type MOs (both with an appreciable platinum 6p character). The latter are deshielding and become pronounced for ligands with the strongest trans influence (they are, however, not operative for σ^p).

In agreement with some recent work for other types of metal-bonded ligand-atom shifts in 5d transition-metal complexes, trans ligand-dependent trends in the SO shifts are affected relatively little by ligand-field energy splittings and more noticeably by changes in the matrix elements of the SO and magnetic-field operators, due to variations in the polarization of the metal d-orbitals by the ligand in trans position. Both σ^p and σ^{SO} contributions to the ^{1}H hydride shielding tensors tend to be dominated by contributions perpendicular to the M−H bond. Overall, the trans ligand affects the covalency of the Pt−H bond but even more decisively the polarization of the metal d-orbitals. For example, good π-acceptor ligands draw the metal orbitals toward them and thereby diminish relevant matrix elements of the ^{1}H hydride shielding tensor. As this influences both paramagnetic and SO contributions to the ^{1}H shieldings in a roughly comparable way, it appears reasonable to view the observed trends in terms of an extended Buckingham−Stephens model that emphasizes the importance of SO effects. Interestingly, ligands with the strongest trans influence (SiR_3, BR_2) are shown to revert the sign of the usually shielding σ^{SO} contribution to the ^{1}H shifts in complexes with partially filled d-shell (by a substantial reduction of the metal 5d-orbital involvement in Pt−H bonding, and by involvement of metal 6p-type orbitals in the magnetic couplings), which counteracts the shielding effect from Pt(d_π) → σ^*(Pt−H)-based couplings and may cause an overall small deshielding of the hydride proton.

Previously observed correlations between the ^{1}H shifts and Pt−H distances arise indirectly from the effect of the trans ligand on the polarization of the metal d orbitals, which in turn affects both the structures and the shifts. For a given complex, changes in the Pt−H distance do not lead to comparable changes in the shift. Correlations between ^{1}H and ^{195}Pt shifts start to break down once more and more systems are included in the comparison. This is due, for example, to much larger SO effects on ^{195}Pt than ^{1}H shifts for heavy halide ligands.

We furthermore noticed a large effect of the exchange-correlation kernel on NMR chemical shifts when substantial SO effects are involved. Clearly, the kernel must be taken into account for accurate relativistic shielding computations, both at the two- and at the four-component level.

ASSOCIATED CONTENT

Supporting Information

Bond lengths in optimized and X-ray structures; Cartesian coordinates of the optimized structures; additional ^{1}H and ^{195}Pt NMR shifts with different methods with and without the exchange-correlation kernel; main contributions from separate excitations to σ^p and σ^{SO} at 2c-ZORA(SO)/PBE0/TZ2P and 1c-PBE/ECP level as well as the appropriate MO plots; background to analysis at one-component perturbation level; absolute ^{195}Pt shieldings. The Supporting Information is available free of charge on the ACS Publications website at DOI: 10.1021/acs.inorgchem.5b00446.

AUTHOR INFORMATION

Corresponding Authors

*E-mail: peter.hrobarik@tu-berlin.de. (P.H.)
*E-mail: martin.kaupp@tu-berlin.de. (M.K.)

Notes

The authors declare no competing financial interest.

ACKNOWLEDGMENTS

Funding from the Berlin DFG excellence cluster on Unifying Concepts in Catalysis (UniCat) is gratefully acknowledged. A.H.G. thanks Fonds der chemischen Industrie for a Ph.D. scholarship. J.A. acknowledges support from Grant No. CHE-1265833 of the National Science Foundation.

REFERENCES

(1) Pidcock, A.; Richards, R. E.; Venanzi, L. M. *J. Chem. Soc. A* **1966**, 1707.
(2) Hartley, F. R. *The chemistry of platinum and palladium: with particular reference to complexes of the elements;* Applied Science Publishers: London, U.K., 1973.
(3) Chatt, J.; Shaw, B. L. *J. Chem. Soc.* **1962**, 5075.
(4) Buckingham, A. D.; Stephens, P. J. *J. Chem. Soc.* **1964**, 4583.
(5) Buckingham, A. D.; Stephens, P. J. *J. Chem. Soc.* **1964**, 2747.
(6) Atkins, P. W.; Green, J. C.; Green, M. L. H. *J. Chem. Soc. A* **1968**, 2275.
(7) Birnbaum, E. R. *Inorg. Nucl. Chem. Lett.* **1971**, *7*, 233.
(8) Ruiz-Morales, Y.; Schreckenbach, G.; Ziegler, T. *Organometallics* **1996**, *15*, 3920.
(9) Hrobárik, P.; Hrobáriková, V.; Meier, F.; Repiský, M.; Komorovský, S.; Kaupp, M. *J. Phys. Chem. A* **2011**, *115*, 5654.
(10) Hrobárik, P.; Hrobáriková, V.; Greif, A. H.; Kaupp, M. *Angew. Chem., Int. Ed.* **2012**, *51*, 10884.
(11) (a) Perdew, J. P.; Burke, K.; Ernzerhof, M. *Phys. Rev. Lett.* **1996**, *77*, 3865. (b) Perdew, J. P.; Burke, K.; Ernzerhof, M. *Phys. Rev. Lett.* **1997**, *78*, 1396.
(12) Adamo, C.; Barone, V. *Chem. Phys. Lett.* **1998**, *298*, 113.

DOI: 10.1021/acs.inorgchem.5b00446
Inorg. Chem. XXXX, XXX, XXX−XXX

(13) Weigend, F.; Ahlrichs, R. *Phys. Chem. Chem. Phys.* **2005**, *7*, 3297.
(14) Andrae, D.; Häußermann, U.; Dolg, M.; Stoll, H.; Preuß, H. *Theor. Chim. Acta* **1990**, *77*, 123.
(15) Peterson, K. A.; Figgen, D.; Goll, E.; Stoll, H.; Dolg, M. *J. Chem. Phys.* **2003**, *119*, 11113.
(16) Turbomole, version 6.3.1, a Development of University of Karlsruhe and Forschungszentrum Karlsruhe GmbH, 1989−2007, Turbomole GmbH, since 2007; available from http://www.turbomole.com.
(17) See, for example, (a) Braunschweig, H.; Brenner, P.; Dewhurst, R. D.; Guethlein, F.; Jimenez-Halla, J. O. C.; Radacki, K.; Wolf, J.; Zöllner, L. *Chem. - Eur. J.* **2012**, *18*, 8605. (b) Cowan, R. L.; Trogler, W. C. *J. Am. Chem. Soc.* **1989**, *111*, 4750. (c) Languérand, A.; Barnes, S. S.; Bélanger-Chabot, G.; Maron, L.; Berrouard, P.; Audet, P.; Fontaine, F. G. *Angew. Chem., Int. Ed.* **2009**, *48*, 6695.
(18) (a) Becke, A. D. *J. Chem. Phys.* **1993**, *98*, 5648. (b) Lee, C.; Yang, W.; Parr, R. G. *Phys. Rev. B: Condens. Matter Mater. Phys.* **1988**, *37*, 785. (c) Stephens, P. J.; Devlin, F. J.; Chabalowski, C. F.; Frisch, M. J. *J. Phys. Chem.* **1994**, *98*, 11623.
(19) *Amsterdam Density Functional (ADF)*, version 2012.01; SCM, Theoretical Chemistry, Vrije Univeriteit: Amsterdam, Netherlands, 2012; available from http://www.scm.com.
(20) van Lenthe, E.; Baerends, E. J. *J. Comput. Chem.* **2003**, *24*, 1142.
(21) Wolff, S. K.; Ziegler, T. *J. Chem. Phys.* **1998**, *109*, 895.
(22) Wolff, S. K.; Ziegler, T.; van Lenthe, E.; Baerends, E. J. *J. Chem. Phys.* **1999**, *110*, 7689.
(23) Wolinski, K.; Hinton, J. F.; Pulay, P. *J. Am. Chem. Soc.* **1990**, *112*, 8251.
(24) Autschbach, J. *Mol. Phys.* **2013**, *111*, 2544.
(25) ReSpect-mDKS, version 3.3.0, 2013; Repisky, M.; Komorovsky, S.; Malkin, V. G.; Malkina, O. L.; Kaupp, M.; Ruud, K., with contributions from Bast, R.; Ekstrom, U.; Knecht, S.; Malkin-Ondik, I.; Malkin, E. (see http://rel-qchem.sav.sk).
(26) Aucar, G. A.; Saue, T.; Visscher, L.; Jensen, H. J. A. *J. Chem. Phys.* **1999**, *110*, 6208.
(27) Kutzelnigg, W. *J. Comput. Chem.* **1999**, *20*, 1199.
(28) Dyall, K. G. *Theor. Chem. Acc.* **2004**, *112*, 403.
(29) Kutzelnigg, W.; Fleischer, U.; Schindler, M. In *NMR—Basic Principles and Progress;* Springer Verlag: Berlin,Germany, p 165.
(30) , Frisch, M. J.; Trucks, G. W., et al. *Gaussian 09,* Revision D.01; Gaussian, Inc.: Wallingford, CT, 2009.
(31) Malkin, V. G.; Malkina, O. L.; Reviakine, R.; Arbuznikov, A. V.; Kaupp, M.; Schimmelpfennig, B.; Malkin, I.; Repisky, M.; Komorovsky, S.; Hrobarik, P.; Malkin, E.; Helgaker, T.; Ruud, K. *MAG-ReSpect,* version 2.3; 2010.
(32) Dolg, M.; Wedig, U.; Stoll, H.; Preuss, H. *J. Chem. Phys.* **1987**, *86*, 866.
(33) Vaara, J.; Malkina, O. L.; Stoll, H.; Malkin, V. G.; Kaupp, M. *J. Chem. Phys.* **2001**, *114*, 61.
(34) Reed, A. E.; Curtiss, L. A.; Weinhold, F. *Chem. Rev.* **1988**, *88*, 899.
(35) Glendening, E. D.; Badenhoop, J. K.; Reed, A. E.; Carpenter, J. E.; Bohmann, J. A.; Morales, C. M.; Weinhold, F. *NBO 5.0;* Theoretical Chemistry Institute, University of Wisconsin: Madison, WI, 2001; available from http://nbo.chem.wisc.edu.
(36) Autschbach, J. *J. Chem. Phys.* **2008**, *128*, 164112.
(37) Bader, R. F. W.; Stephens, M. E. *J. Am. Chem. Soc.* **1975**, *97*, 7391.
(38) Fradera, X.; Austen, M. A.; Bader, R. F. W. *J. Phys. Chem. A* **1999**, *103*, 304.
(39) Kohout, M. *DGrid*, version 4.6; Springer: Germany, 2011; available from http://www2.cpfs.mpg.de/~kohout/dgrid.html.
(40) Nakajima, T.; Hirao, K. *Chem. Rev.* **2012**, *112*, 385.
(41) Klamt, A.; Schüürmann, G. *J. Chem. Soc., Perkin Trans. 2* **1993**, 799.
(42) Hartley, F. R. *Chem. Soc. Rev.* **1973**, *2*, 163.
(43) Engesser, T. A.; Hrobárik, P.; Trapp, N.; Eiden, P.; Scherer, H.; Kaupp, M.; Krossing, I. *ChemPlusChem* **2012**, *77*, 643 and references therein .
(44) Voigt, J.; Braun, T. *Dalton Trans.* **2011**, *40*, 12699.
(45) Stahl, S. S.; Labinger, J. A.; Bercaw, J. E. *Inorg. Chem.* **1998**, *37*, 2422.
(46) Appleton, T. G.; Chisholm, M. H.; Clark, H. C.; Manzer, L. E. *Inorg. Chem.* **1972**, *11*, 1786.
(47) Schreckenbach, G. *Theor. Chem. Acc.* **2002**, *108*, 246.
(48) van Lenthe, E.; Snijders, J. G.; Baerends, E. J. *J. Chem. Phys.* **1996**, *105*, 6505.
(49) For halogen dependence of NMR shifts, see, for example: Engesser, T. A.; Hrobárik, P.; Trapp, N.; Eiden, P.; Scherer, H.; Kaupp, I. *ChemPlusChem* **2012**, *77*, 643 and references therein. .
(50) Autschbach, J.; Zheng, S.; Schurko, R. W. *Concepts Magn. Reson., Part A* **2010**, *36A*, 84.
(51) Dean, R. R.; Green, J. C. *J. Chem. Soc. A* **1968**, 3047.
(52) Garbacz, P.; Terskikh, V. V.; Ferguson, M. J.; Bernard, G. M.; Kędziorek, M.; Wasylishen, R. E. *J. Phys. Chem. A* **2014**, *118*, 1203.
(53) Vícha, J.; Straka, M.; Munzarová, M. L.; Marek, R. *J. Chem. Theory Comput.* **2014**, *10*, 1489.
(54) Kaupp, M. In *Relativistic Electronic Structure Theory II: Applications;* Schwerdtfeger, P., Ed.; Elsevier: Amsterdam, 2004; p 552.
(55) Pyykkö, P.; Görling, A.; Rösch, N. *Mol. Phys.* **1987**, *61*, 195.
(56) Vícha, J.; Foroutan-Nejad, C.; Pawlak, T.; Munzarová, M. L.; Straka, M.; Marek, R. *J. Chem. Theory Comput.* **2015**, *11*, 1509.
(57) Manninen, P.; Ruud, K.; Lantto, P.; Vaara, J. *J. Chem. Phys.* **2005**, *122*, 114107.
(58) Manninen, P.; Ruud, K.; Lantto, P.; Vaara, J. *J. Chem. Phys.* **2006**, *124*, 149901.
(59) Manninen, P.; Lantto, P.; Vaara, J.; Ruud, K. *J. Chem. Phys.* **2003**, *119*, 2623.
(60) Autschbach, J.; Zheng, S. *Magn. Reson. Chem.* **2008**, *46*, S45.
(61) Sterzel, M.; Autschbach, J. *Inorg. Chem.* **2006**, *45*, 3316.
(62) Truflandier, L. A.; Sutter, K.; Autschbach, J. *Inorg. Chem.* **2011**, *50*, 1723.

DOI: 10.1021/acs.inorgchem.5b00446
Inorg. Chem. XXXX, XXX, XXX−XXX